Conversion among North Atlantic surface water types

By KEVIN G. SPEER, *IFM Kiel, Düsternbrooker Weg 20, D-2300 Kiel 1, Germany**

ABSTRACT

Climatological data sets are used to estimate the amount of water changing temperature and salinity at the sea-surface owing to air-sea exchanges. Considering this conversion as a function of sea-surface temperature and salinity leads to the definition of a conversion vector, which represents mass sources and sinks for each water type. The vector representation shows graphically the way the shape of the temperature-salinity relation is driven at the surface by the air-sea heat and fresh water fluxes.

1. Introduction

Charts of the geographical distribution of air-sea heat exchange show regions of strong heat gain and heat loss by the ocean, associated with the conversion of water to cooler or warmer temperatures. Charts of evaporation minus precipitation may be used similarly to infer changes in salinity at the sea surface. Such information has provided the basic picture of strong net cooling along the Gulf Stream, the heating of equatorial and coastal upwelling regimes, and the strong evaporation over the southern subtropical gyre north of the intertropical convergence zone (see, e.g., Schmitt et al., 1989). These general features of air-sea exchange generate special types of sea-water, that is, water within recognizable temperature and salinity bounds. Examples of special water types include the warm water pool of the western tropics (26–30°C, 34–36°/$_{oo}$), the salinity maximum water of the southern subtropical gyre (20–25°C, >37°/$_{oo}$), and subtropical mode water (near 18°C and 36.5°/$_{oo}$), (Fig. 1; Wright and Worthington, 1970).

The description of the thermohaline forcing in geographical coordinates while the response (e.g., mode water) is described in temperature-salinity coordinates makes the connection between the two indirect and difficult to analyse. To make this connection clearer one may examine air-sea fluxes as a function of surface water properties instead of as a function of position. Then it becomes natural to consider the air-sea exchanges from the point of view of their distribution over sea-surface temperature and salinity classes, that is, surface water type. The basis for such a description is presented here together with estimates of conversion for the surface water of the North Atlantic Ocean.

2. Conversion

The amount of heat required to raise F^T grams of water ΔT (°C) is Q (J):

$$F^T C_p \, \Delta T = Q. \tag{1}$$

Conversely, F^T is the amount of water converted from T to $T + \Delta T$ for a given Q. Consider the outcrop area encompassed by the band $T \pm \Delta T/2$ at the sea-surface. By specifying the temperature change to be that separating the bands (ΔT), the amount of mass converted from one band to another is determined by the total heat source to a band.

To find this heat source substitute $Q = \mathcal{H} \, \mathrm{d}A \, \mathrm{d}t$, where $\mathcal{H}$ is the heat flux over the sea-surface area element $\mathrm{d}A$ during a time interval $\mathrm{d}t$, and sum over all area elements which are within the temperature range $T \pm \Delta T/2$. Or, more generally, to find $F^T(S, T)$ average the air-sea transformation Q/C_p over the sea-surface area defined by the intersection of the two bands $T \pm \Delta T/2$ and $S \pm \Delta S/2$:

$$F^T(S, T) \, \Delta t = \int_{\text{year}} \int_{\text{area}} \frac{\mathcal{H}}{C_p} \frac{\Pi(T - T')}{\Delta T}$$

$$\times \frac{\Pi(S - S')}{\Delta S} \, \mathrm{d}A \, \mathrm{d}t, \tag{2}$$

* Now at: Laboratoire de Physique des Océans, IFREMER, B.P. 70, 29280 Plouzané, France.

where Π is the boxcar sampling function, with the value 0 when either the temperature or salinity is outside the given range, or 1 when they are within. The distribution of T and S at the surface shows extrema (e.g., Fig. 1), so that outcrop intersections at a given temperature and salinity are not necessarily adjacent.

Note that in terms of temperature alone one can write:

$$F^T(T) \, C_p \, dT = dQ(T)$$

or

$$F^T(T) = \frac{1}{C_p} \frac{dQ}{dT}, \tag{3}$$

where $dQ(T)$ is the heat input in a small band around the T isotherm. Except for a factor of ρ this is Walin's (1982) expression for the volume flux

across isotherms $(\rho C_p)^{-1} \, dQ/dT$ driven by a surface heat flux.

In the above integration, the boxcar sampling of the sea-surface keeps track of the salinity S and temperature T at which the conversion occurs. The units are mass per salinity bin: $g/^o/_{oo}$. Dividing by a Δt of one year times the surface density gives the yearly average volume transport in $m^3 \, s^{-1}/^o/_{oo}$.

The fresh water *mass* flux $\mathscr{W}$ (evaporation minus precipitation) has an analogous effect. To see how, consider adding M grams of fresh water to X g of seawater at salinity S, which becomes $X + M$ g at salinity $S - \Delta S$. Then conservation of salt implies that $XS = (M + X)(S - \Delta S)$, or $X + M = MS/\Delta S$. With $F^S \, \Delta t = X$ (ignoring M by comparison), one can therefore write to a good approximation $\Delta(F^S S) = 0$, and substitute $\Delta F^S = -\mathscr{W} \, dA \, dt$ to get:

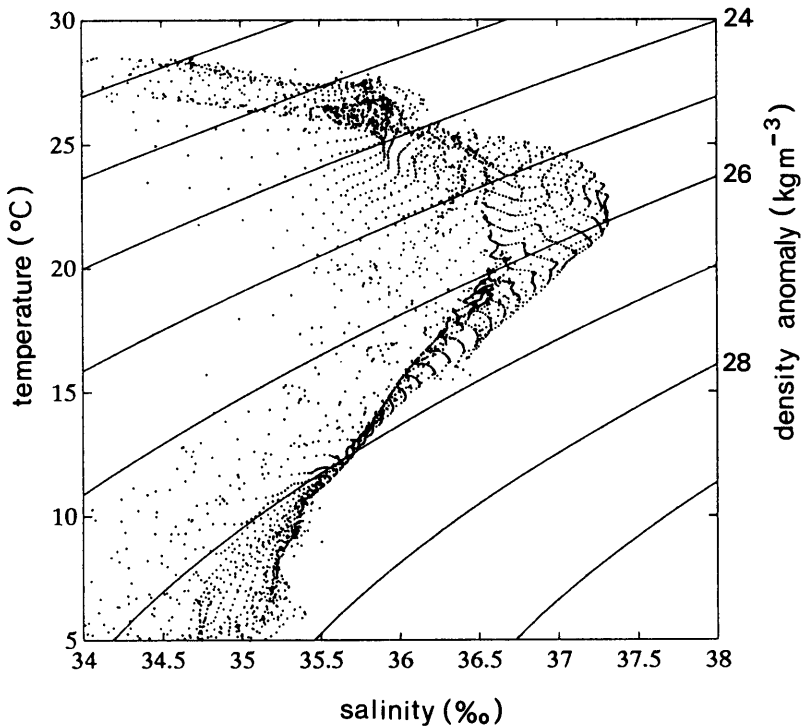$$F^S \, \Delta S = S\mathscr{W} \, dA \, dt. \tag{4}$$

Fig. 1. Temperature-salinity diagram for the February sea-surface according to the Levitus (1982) North Atlantic climatology. Each point represents a $1°$ by $1°$ square at the surface. A large area of warm water ($T > 25$) occurs, tailing off to low salinity owing to river outflow. The salinity maximum is cooler ($20 < T < 25$), and denser. From $10–15°C$ Central Water is exposed at this time of the year in the northern subtropical gyre; at cooler temperatures a wide variety of types occur in the interior and boundary regions of the subpolar gyre.

Here the surface fresh water source has been used to find the rate at which seawater changes salinity from S to $S + \Delta S$, or, in other words, the amount of seawater per unit time which is required to mix with the fresh water source to change salinity by ΔS. Thus the haline part of the conversion at the surface water type S, T is:

$$F^S(S, T)\, \Delta t = \int_{\text{year}} \int_{\text{area}} S \mathscr{W} \frac{\Pi(T - T')}{\Delta T}$$

$$\times \frac{\Pi(S - S')}{\Delta S}\, \mathrm{d}A\, \mathrm{d}t. \tag{5}$$

From these two quantities define the conversion vector, which is used below:

$$F(S, T) = (F^S, F^T). \tag{6}$$

If salinity is eliminated from the temperature component by integrating over all S, the result $F^T(T) = \int F^T(S, T)\, \mathrm{d}S$ is equivalent to the net cross-isotherm mass flux calculation proposed by Walin (1982) and carried out by Andersson, et al. (1982; their $\mathrm{d}Q/\mathrm{d}T$). This was checked by integrating once more with respect to temperature and comparing the resulting Q function with their result; the agreement is close but not exact since the data sources are different. Both cross-isotherm and cross-isohaline transfers were discussed by Tziperman (1986) in the context of the cross-isopycnal mass flux as a function of density and the associated formation in density classes. Individually they represent the amount of mass crossing an isotherm per $^\circ/_{oo}$ in one year and the amount of mass crossing an isohaline per $^\circ$C in one year. While Andersson et al. (1982) focussed on temperature coordinates and Tziperman (1986) on density coordinates the point here is to view these quantities as functions of both temperature and salinity.

The conversion vector $F = (F^S, F^T)$ points in the direction of change for each water type on the $S - T$ plane. Some conversion will change T and S but preserve the initial density of the water (F tangent to isopycnals on the $S - T$ plane) and some conversion will change the density of the water. To discriminate between the two one may examine the component of F across an isopycnal in the $S - T$ plane $F(S, T) = F \cdot \nabla\rho/|\nabla\rho|$. This expression is a generalization of the cross-isopycnal mass flux discussed by Tziperman (1986) to the $S - T$ plane, which is recovered if the cross-isopycnal component $F(S, T)$ is itself integrated along curves of constant density (Speer and Tziperman, 1992).

Knowing the amount of water transformed from one water type to another allows the net amount formed to be calculated: the convergence $-\nabla \cdot F$, where

$$\nabla = \left(\Delta S \frac{\partial}{\partial S}, \Delta T \frac{\partial}{\partial T} \right)$$

is the amount of water deposited or removed as a result of the air-sea fluxes at a given temperature and salinity. Of special interest is the formation which results only from cross-isopycnal transfers $\partial F(S, T)/\partial\rho$, or,

$$M(S, T) = \nabla F(S, T)\, \nabla\rho/|\nabla\rho|, \tag{7}$$

because such transfers are more likely to generate water masses of well-defined temperature and salinity characteristics.

3. Application

The vector field F has been calculated for the range of surface temperature and salinity found in the Levitus (1982) atlas for the North Atlantic. The strongest conversion occurs in the subrange $34–38^\circ/_{oo}$ and $5–30^\circ$C illustrated here (Fig. 2), where each component has been multiplied by the bin width ΔS or ΔT to get units of transport. (This quantity is no longer a local one on the $S - T$ plane, since it must be defined over a water type outcrop of finite area).

Each position in the plane from which a vector originates consists of a given water type, whose area $\Delta S\, \Delta T$ is large enough to get a reasonably coherent annual average. The smallest intervals used to make the calculation were 0.5°C and $0.1^\circ/_{oo}$ as smaller choices are not consistent with the 1° spatial resolution of the hydrographic data set used here (Levitus, 1982). That is, smaller choices may be associated with outcrop areas of dimensions smaller than a 1° box. The heat flux and evaporation used in the calculation are from Isemer and Hasse (1987); precipitation estimates were provided by C. Dorman (see Schmitt et al., 1989). Fresh water sources and sinks at the ocean
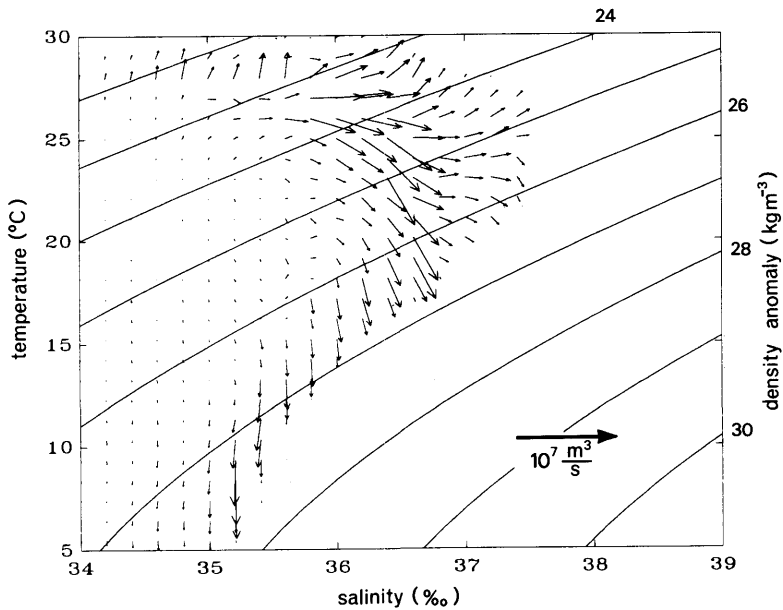
Fig. 2. Conversion diagram showing the vector field F on a portion of the temperature-salinity plane, over $1°C$ by $0.2°/_{oo}$ classes. Density anomaly σ_t $(kg\ m^{-3})$ is superimposed.

boundary, including river inflow and marginal sea contributions, are neglected. All data except sea-surface salinity were monthly; the salinity was linearly interpolated to monthly values. Only annual average results are presented here.

The overall shape or envelope of the surface conversion is simply that of a surface $T - S$ scatter diagram, since conversion occurs only on the surface outcrop of a given water type. The magnitude of the conversion is governed by the exposed surface area of water within a given $S - T$ range and the strength of the air-sea fluxes affecting that water. The conversion vector shows transformations at the surface in every direction, but with only a tiny amount corresponding to both a warming and freshening. The general trend is an outward transfer of water away from a broad area of the $T - S$ plane surrounding $20°C$ and $35°/_{oo}$ toward the outer $T - S$ property limits of surface water. In other words warm water is heated, salty water salinified, and cool water cooled, which creates the impression that the surface mixed layer $T - S$ characteristics are evolving toward higher salinities and both greater and lesser temperatures. A number of processes constrain this tendency, including mixing, which returns water toward the inside of the diagram, evaporative cooling,

which limits the warmest water temperatures, and sinking, which removes water from the surface.

Conversion is evident both along and across curves of constant density. The convergence $(-\nabla \cdot F,$ not shown) basically shows negative values on the inner side of the largest transformation vectors, and positive values on the outer side, corresponding to both production and removal of water from a given water type. The cross-isopycnal formation $M(S, T)$ (Fig. 3) has a similar form, and illustrates how the transformations which change density converge and diverge over the $S - T$ plane. Major maxima are located roughly at the subtropical mode water type ($18°C$ and $36.5°/_{oo}$), along a ridge leading from this water type toward $4°C$ and $35°/_{oo}$, a range of salinities near $28°C$, and a water type near $21°-24°C$ and $36.5°/_{oo}$. The strongest divergence removes water from the temperature and salinity classes near $27°$ and $36°/_{oo}$. The correspondance with the vector field can only be rough as some smoothing was necessary for visualization, which more than halved the resolution specified above. For a steady state these divergences and convergences are balanced by mixing, either at or below the surface (Walin, 1982).

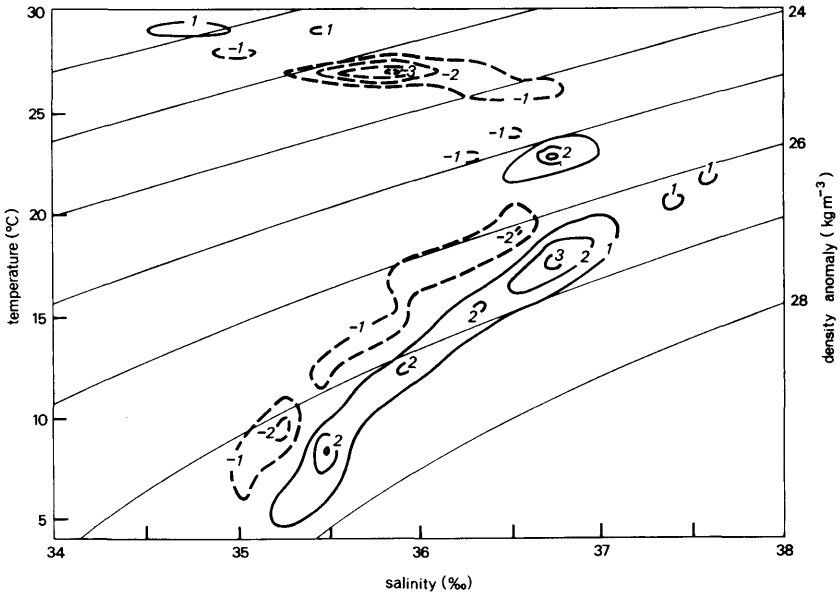It is natural to compare these results to the

Fig. 3. Smoothed cross-isopycnal formation $\partial F(S, T)/\partial \rho (\times 10^6 \, \mathrm{m^3 \, s^{-1}})$.
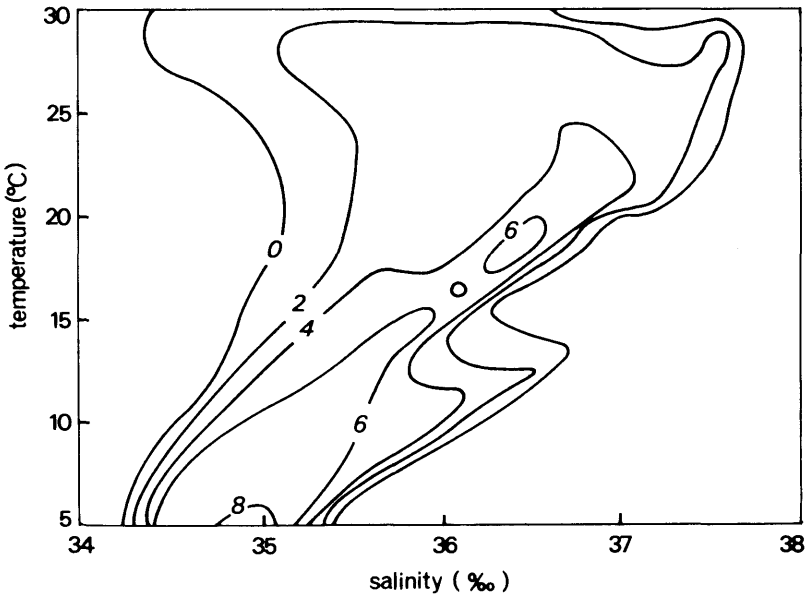

Fig. 4. Logarithm of volume in units of $10^3 \, \mathrm{km^3}$ from Wright and Worthington (1970), over $1\,°\mathrm{C}$ by $0.2°/_{oo}$ classes. Volumes at temperatures warmer than $20\,°\mathrm{C}$ were interpolated from $2\,°\mathrm{C}$ intervals to $1\,°\mathrm{C}$ intervals, while the finer divisions between $4\,°\mathrm{C}$ and $10\,°\mathrm{C}$ were summed over $1\,°\mathrm{C}$ intervals.

volumetric census of Wright and Worthington (1970), to see how well correlated the distribution of volume over water type is with the surface formation of a particular water type. The connection between the two observations is not exactly direct, though, since it is likely that the mixing processes responsible for maintaining the steady state together with large-scale dynamics control the volume distribution in ways that depend sensitively on other aspects of the circulation as well.

Over the water warmer than 4°C the volume distribution varies by three orders of magnitude, and so the logarithm of volume was calculated for easier comparison (Fig. 4). Unfortunately many significant details of the distribution are invisible on such a plot; on the other hand, the resolution of M shown here is itself coarse, being no better than 1°C by 0.2°/$_{oo}$. A ridge of high volume and of formation are roughly aligned (Figs. 3, 4), but with a slight offset toward saltier or cooler values, which may be a problem of resolution. Surface fluxes create a sink over much of the water near 25°C, and volumes are smaller there than along the main ridge of Central Water. At slightly warmer temperatures M is positive, and a weak volume maximum occurs (between 34.4°/$_{oo}$ and 36°/$_{oo}$, Wright and Worthington, 1970). The most striking difference between the diagrams, however, is the absence of formation over the saline extension of volumetric classes near 12°C. This extension is due to the influence of Mediteranean Water, which injects warm, saline water into the interior. To account for this water the calculation must be extended to include the Mediteranean Sea.

Quantitative conversion estimates such as this one seem likely to constrain the strength of mixing between various water masses, particularly if they can be used in combination with tracer studies. The reason is that tracer studies are often designed to yield estimates for the ventilation of renewal of water masses at various levels or densities. Yet tracer concentrations in the ocean represent a mix of surface conversion and surface and interior mixing processes, and thus so do the resulting ventilation estimates. The conversion rates calculated here, on the other hand, are in principle distinct from (and opposite to) those of mixing (although of course in practice the accuracy of the data can be questioned and the resolution of the data is coarse, representing an average over smaller space and time scales). Therefore the combination of mass source estimates (like $M(S, T)$) with tracer distributions could help to separate processes and determine the intensity of mixing.

4. Discussion

The relation between conversion and surface flow is not direct. A qualitative example may be used to show how the connection between the two can be made, and under which circumstances it breaks down. Walin (1982) provided a formalism for distinguishing between surface and interior cross-isothermal flow, and argued that the large outcrop areas (surface area between specified isotherms) of warm water give rise to a turbulent heat flux divergence large enough to overwhelm the surface heating and produce a net heat loss to water near the surface. This permits a cross-isothermal flow toward cooler water, while horizontal advection can balance surface cooling directly in regions of mean heat loss. This scenario links the sinking regions to the warm water pool, which ultimately supplies them with mass. The driving force is the pressure gradient associated with the surface density differences.

Away from the equator rotation tends to make the flow parallel to the pressure (and density) field, except in the Ekman layer. The flow across temperature and salinity surfaces in a surface layer is generated by the net divergence of fluxes across the layer. If one ignores horizontal mixing and insulates the surface layer from the interior, then flow on the conversion diagram corresponds to flow in the surface layer. One may trace back the origin of this surface conversion to the inner, upstream, part of the diagram.

A crude illustration of the source region can be obtained by plotting the position of all water types within the box $T = 20 \pm 5$°C and $S = 34.8 \pm 0.8$°/$_{oo}$. These water types are not found everywhere in the interior of the North Atlantic, but in two special regions: the Slope Water along the North American continent and along the North Atlantic Drift, and in upwelling regions off Africa and along the equator (Fig. 5). Other water types are present as well in these source regions, as conversion (and mixing) create new types from old. This distribution of source regions locates the lateral supply to the warm water pool in the equatorial and coastal upwelling regions, and
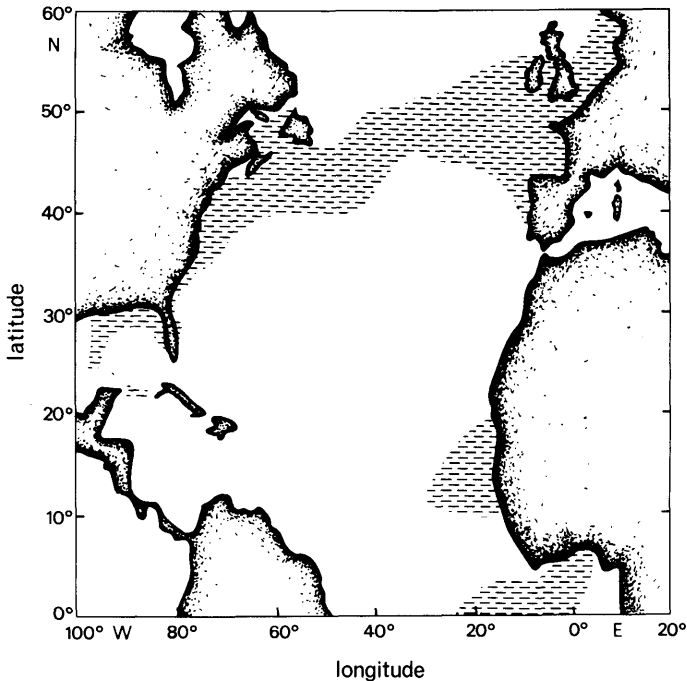
K. G. SPEER

Fig. 5. Location of surface temperature-salinity characteristics at any time of year on the inner, divergent, side of the conversion diagram (see text).

illustrates the Slope Water and North Atlantic Drift origin of the mode waters of the subtropical and subpolar gyre in the surface-advection limit. Thus the conversion diagram reproduces, from a somewhat different perspective, expectations about the movement of surface water in the subtropical and subpolar gyres and under the influence of the Trades, modified by cooling in the former and heating in the latter.

To investigate the part of the surface cross-isothermal and cross-isohaline flow driven by mixing requires detailed information about the distribution of temperature and salinity within the ocean. Although in a steady-state the conversion shown on the diagram is balanced by an equal and opposite conversion due to mixing, without a knowledge of where this mixing occurs one cannot identify conversion with actual flow in the ocean. Walin's (1982) division of turbulent fluxes into surface and interior component addresses this problem but doesn't distinguish the responsable mechanisms or their length and time scales. Niiler and Stevenson (1982) considered the heat balance

of the warm water pool and concluded that vertical turbulent heat transport by small-scale motion can balance the net surface heating, while horizontal mixing is relatively weak. They did not try to resolve the intensity of mixing on separate temperature surfaces, but used an average figure for the tropical thermocline. Multiplying this average intensity (estimated at 6–20 W/m^2) by the outcrop area gives the net heat divergence between two such surfaces. This can amount to a strong cooling at the outer edge of the pool, perhaps larger than the total surface heating of the outcrop region for certain temperature ranges.

Exactly how all the processes involved in the formation of water masses are related to each other and to the circulation is a difficult question, though. Both mixing and air-sea fluxes are controlled to some extent by the circulation, and in turn exert a controlling influence themselves. Thus, while estimates of formation rates such as those presented here should help to infer the integrated effect of mixing, a detailed understanding of the strength and distribution of mixing may depend

sensitively on the dynamics of the circulation. Perhaps it helps to describe this interrelation the other way around: the ocean is subject to dynamical constraints which are built in to the surface temperature, salinity, and fluxes. The way these constraints operate and their degree of control over conversion has not been addressed. Nevertheless, mass source information for each water type, perhaps in combination with other tracer data, should help to constrain estimated of mixing.

5. Acknowledgements

REFERENCES

Andersson, L., Rudels, B. and Walin, G. 1982. Computation of heat flux through the ocean surface as a function of temperature. *Tellus 34*, 196–198.

Isemer, H.-J. and Hasse, L. 1987. *The Bunker climate atlas of the North Atlantic Ocean, vol. 2: Air-sea interactions.* Springer-Verlag, Berlin, 218 pp.

Levitus, S. 1982. *Climatological atlas of the world ocean.* NOAA Professional Paper 13, National Oceanic and Atmospheric Administration, Rockville, Maryland, 173 + XV pp.

Niiler, P. P. and Stevenson, J. 1982. The heat budget of tropical ocean warm water pools. *J. Mar. Res. 40* (suppl.), 465–480.

Schmitt, R. W., Bogden, P. S. and Dorman, C. E. 1989. Evaporation minus precipitation and density fluxes for the North Atlantic. *J. of Phys. Ocean. 19*, 1208–1221.

Speer, K. and Tziperman, E. 1992. Rates of water mass formation in the North Atlantic Ocean. *J. Phys. Ocean. 22*, 94–104.

Tziperman, E. 1986. On the role of interior mixing and air-sea fluxes in determining the stratification and circulation of the oceans. *J. of Phys. Ocean. 16*, 680–693.

Walin, G. 1982. On the relation between sea-surface heat flow and thermal circulation in the ocean. *Tellus 34*, 187–195.

Wright, W. R. and Worthington, L. V. 1970. The water masses of the North Atlantic Ocean; a volumetric census of temperature and salinity. *Serial atlas of the marine environment*, folio 19, American Geographical Society, New York, 8 pp. and 7 plates.